



**HAL**  
open science

# Organic glass-forming liquids and the concept of fragility

Christiane Alba-Simionesco

► **To cite this version:**

Christiane Alba-Simionesco. Organic glass-forming liquids and the concept of fragility. Comptes Rendus. Physique, In press. hal-03876693

**HAL Id: hal-03876693**

**<https://hal.science/hal-03876693>**

Submitted on 28 Nov 2022

**HAL** is a multi-disciplinary open access archive for the deposit and dissemination of scientific research documents, whether they are published or not. The documents may come from teaching and research institutions in France or abroad, or from public or private research centers.

L'archive ouverte pluridisciplinaire **HAL**, est destinée au dépôt et à la diffusion de documents scientifiques de niveau recherche, publiés ou non, émanant des établissements d'enseignement et de recherche français ou étrangers, des laboratoires publics ou privés.



# Organic Glass-Forming Liquids and the Concept of Fragility

Christiane Alba-Simionesco<sup>a</sup>

<sup>a</sup> Laboratoire Léon Brillouin, Université Paris-Saclay, CEA, CNRS, 91191, Gif-sur-Yvette, France

E-mail: [christiane.alba-simionesco@cea.fr](mailto:christiane.alba-simionesco@cea.fr) (C. Alba-Simionesco)

## Abstract.

An important category of glass-forming materials is organic; it includes molecular liquids, polymers, solutions, proteins that can be vitrified by cooling the liquid under standard conditions or after special thermal treatments. The range of applications is large from materials to life sciences and recently to electronics. To distinguish them from other systems described in this issue, some specific properties such as the range of their glass transition temperature ( $T_g$ ), their ability to vitrify and some rules of thumb to locate  $T_g$  are presented. The most remarkable property of these liquids is how fast in temperature their viscosity or structural relaxation time increases as approaching  $T_g$ . To characterize this behavior and rank the liquids of different strength, C.A. Angell introduced the concept of Fragility nearly 40 years ago. He proposed to classify liquids as fragile or strong in an Arrhenius plot with  $T_g$  scaling (the strongest ones have never been observed in organic glasses, except for water under specific conditions). The  $T_g$  value and the fragility of a given liquid can be changed by applying pressure, *i.e.* changing the density. One can then explore the properties of the supercooled/overcompressed liquid and the glass in a  $P - T$  phase diagram. The  $T_g$  line corresponds to an isochronic line, *i.e.* a line at constant relaxation time with different pairs of density-temperature. We observe that all data can be placed on master-curves that depend only on a single density- and species-dependent and T-independent effective interaction energy,  $E_\infty(\rho)$ . An isochoric fragility index is defined as an intrinsic property of a given liquid, that can help in rationalizing all the correlations between the glass properties below  $T_g$  and the viscous slowing down just above  $T_g$  from which they are made. Geometrical confinement of liquids is also a way to modify the dynamics of a liquid and the properties of a glass; it corresponds to a large number of situations encountered in nature. Another phase diagram  $T - d$  ( $d$ = pore diameter) can be defined with a non-trivial pore size dependence of the glass transition, which is also strongly affected by surface interactions.

**Keywords.** molecular liquids and glasses, polymers, fragility, density scaling, correlations.

This article is a draft (not yet accepted!)

## 1. Introduction

The qualification of glass applies to any system from simple liquids to foams, colloids and granular materials, for which structurally arrested states are observed when approaching their glass transition. They all exhibit a growingly slow and heterogeneous dynamics while below the transition the solids made displays out-of-equilibrium behavior with a strong dependence on thermal history. A wide variety of systems can fall into this category described as « a frozen beauty » by C.A. Angell [1]. As pointed out by J. Dyre [2], the phenomenon is so universal that the "glassy"

state can be considered as the fourth state of matter requiring a combination of theoretical approaches of solid and liquid states; likewise, its experimental study needs the combination of many techniques and observables over a large temporal and spatial range. The most common way to obtain a glass is to cool a liquid at atmospheric pressure. However it is certainly not the only way to form a glass. As shown in [1] many other routes are possible as long as crystallization is prevented: various procedures of vapor deposition on a cold substrate, binary solutions, amorphisation by milling widely used in pharmacology [34], compression and cooling to change the density of the liquid, or confinement at nanoscale.

Among all classes of glasses, organic glasses, (*i.e.* with Carbon in their chemical formula, and Hydrogen, Oxygen, Nitrogen..) are of special importance, and play a major role in several applications in chemistry or biology. Recently the understanding of their electronic structure and properties became a key parameter for the design of high performance optical and electronic devices, like organic light emitting diodes [3]. However, for all these applications, it remains important to determine the factors driving the formation of glass and the consequences on its properties. Glassforming liquids can be molecular, ionic, liquid crystals, polymer melts or binary-ternary solutions. Many features of the rich phenomenology associated with the glass formation can be also observed in solid materials such as plastic crystals (glassy crystals [4]) or low temperature quadrupolar glasses, out of scope here. The Glass Transition is not a genuine thermodynamic phase transition toward a rigid state. The exact definition of  $T_g$  is arbitrary and corresponds to the temperature at which the very slow relaxation dynamics of a supercooled liquid looks finally stopped at a given experimental time, then the system falls out of equilibrium and becomes a glass. Quantitatively, several more or less equivalent definitions of  $T_g$  can be found in the literature depending on the experiments: one can define it on cooling as the temperature at which the structural relaxation time  $\tau_\alpha$  reaches 100s or 1000s, or the viscosity  $10^{11} - 10^{13}$  poises; alternatively, on cooling and heating,  $T_g$  is the temperature at which a jump in the heat capacity versus  $T$  is observed. The latter definition of  $T_g$  is usually easily accessible over a narrow temperature range from standard calorimetric scanning measurements (DSC), a very common laboratory technique, for cooling and heating rates between 1 – 20 K/min. When the liquid is cooled at constant pressure, the change of the dynamical properties is so large that it requires an Arrhenius (logarithmic) representation involving an effective activation energy: for organic liquids typically the change of the relaxation time at atmospheric pressure is about 14 orders of magnitude, from the boiling temperature  $T_b$  close to the picosecond to  $T_g$  as defined above. For the viscosity, the dynamical range is similar but, in the highly viscous regime, it depends on the temperature dependence of the elastic shear modulus  $G_\infty$  which differs from one liquid to another [5]. This drastic T-dependence can be decomposed in a first Arrhenius-like behavior at high temperature, slightly above the melting temperature with an almost constant activation energy (with a weak density dependence); then, below a given temperature  $T^*$  [6] in the supercooled regime, *i.e.* below the melting temperature, a super-Arrhenius behavior is observed with a temperature dependent activation energy:

in the liquid state, with  $E_\infty$  roughly constant [7],  $\tau(T) = \tau_\infty \exp\left(\frac{E_\infty}{T}\right)$ ,

in the supercooled regime,  $\tau(T) = \tau_\infty \exp\left(\frac{E(T)}{T}\right)$

with  $E(T)$  growing as  $T$  decreases and empirically defined as  $E(T) = k_B T^* \ln(\tau(T, P_{atm})/\tau_\infty)$ .

Figure 1 left schematically illustrates the viscous slowing down of a molecular (organic) liquid with characteristic temperatures: three are experimentally defined ( $T_b$ ,  $T_m$ ,  $T_g$ ), two are theoretically defined and experimentally avoided ( $T^*$  from the Frustration Limited Domain Theory,  $T_c$  from the Mode Coupling Theory), two are extrapolated and unreachable ones ( $T_o$ , the temperature at which  $\eta$  or  $\tau_\alpha$  might diverge,  $T_K$ , the Kauzmann temperature where the liquid configurational entropy vanishes). In Figure 1 right is represented the combination of

experimental spectroscopic and scattering techniques required for the study of the viscous slowing down of a molecular liquid (note that for each techniques specific equipments and various methods must be implemented). The degree of departure from an Arrhenius temperature dependence is often quantified from one system to another one by the fragility index  $m$  proposed by Austen Angell almost twenty years ago. The fragility or steepness index is commonly defined at  $T_g$ , *i.e.* at long time scales, by  $m = \partial \log_{10}[\tau(T)/\tau_\infty] / \partial(T_g/T)|_{T_g}$ . The usefulness and the robustness of the concept were addressed several times by various authors [8] and nowadays it remains an important criterium to classify systems.

The supercooled regime is also characterized by a non-exponential time dependence of the relaxation function, whatever is the technique or the liquid; therefore one cannot consider a single relaxation time but an averaged one, that might span over few decades in time between the fast and the slowest ones. Many debates took place to understand what this stretching of the relaxation function could say about the nature of the dynamics of supercooled liquids. In the 90's several experimental results, using very different observables, allowed to clarify and qualify as heterogeneous the nature of the dynamics. One step further was to consider it as spatially heterogeneous and introduce the notion of supramolecular dynamical length scale [9], which can not be detected in the pair correlation function defined by the static structure factor.

Finally, a third characteristic of the supercooled liquid is of thermodynamic nature; from specific heat measurements, one can calculate the variation of an excess entropy  $S_c$  defined as the difference between the entropy of the liquid and the corresponding crystal from the melting temperature down to below  $T_g$ . As pointed out by Kauzmann [10], it decreases very rapidly below  $T_m$  and might even become negative by extrapolation well below  $T_g$  (known as the Kauzmann paradox). This excess entropy and its T-dependence are nicely correlated to the viscosity changes in the Adam-Gibbs model [12] allowing to link dynamics and thermodynamics ; it predicts a second-order phase transition when  $S_c = 0$  at  $T = T_{Kauzmann}$  with a diverging relaxation time. Many theories of the glass transition [11], are relying on this approach even if not fully supporting the original Adam-Gibbs model. Therefore the description of the dynamics with the above equations supposes thermally activated processes with a T-dependence of the activation energy being due to the growth of a length scale of structural or dynamical origine as temperature decreases (see other articles in this issue) and the final cancelling of configurational entropy of liquid suggesting that a thermodynamic phase transition underlies the glass transition.

The search for such a length is subject of many experimental investigations; its experimental determination remains very difficult, indirect and limited to few methods. However a major step has been taken with the observation of its growth when T decreases by Ladieu et al [13]. These results, observed for several systems, are in agreement with the fact that a length would be responsible for the viscous slowing down. Unfortunately its relationship with any structural analogue remains an open question.

It should be noted that this description of viscous slowing down is not the only one. There are other theoretical approaches and models that do not refer to a particular length, such as the free volume theory and the mode coupling theory (MCT) or the shoving model [14] ( even if it was demonstrated in the case of the MCT that a length scale exists [15]). Moreover, adding to the complexity of the phenomenon, several other lengths have been identified bearing the signature of disorder in the glassy state close to  $T_g$  and low temperature anomalies : in the GHz-THz frequency domain , one can define characteristic lengths from elastic heterogeneities , plastic deformation, the relative strength of shear and bulk moduli, or the ratio of the transverse sound velocity to the boson peak frequency [16], any property defining a length scale at which the continuum elastic description breaks down .

The above description corresponds to the formation of a glass on cooling under standard isobaric conditions, *i.e.* at atmospheric pressure for experiments versus isochoric conditions for the-

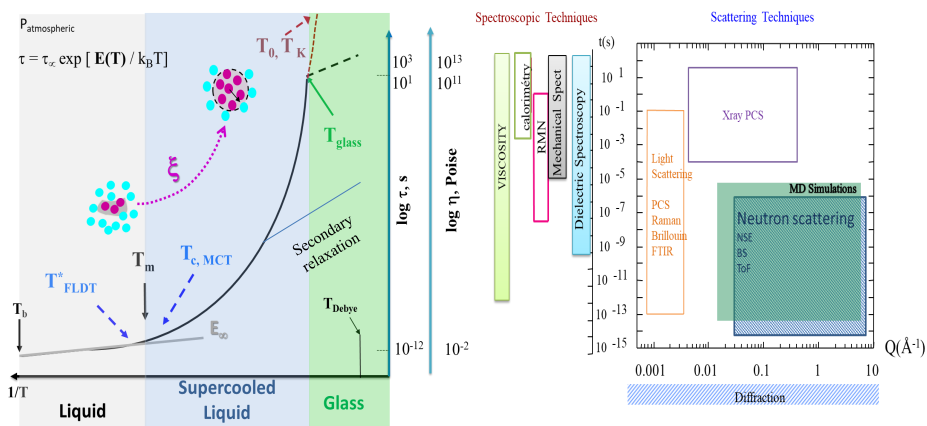


**Figure 1.** left: Schematic representation of the viscous slowing down of molecular liquids at atmospheric pressure from the boiling point at  $T_b$  to the Glass transition temperature  $T_g$ . Three dynamical regimes are defined with a different color code, light blue, stable liquid, dark blue supercooled liquid, green for glass. Characteristic temperatures describing the viscous slowing down in the literature are added and an increased correlation length is schematically represented; right: spectroscopic and scattering techniques required for the study of the viscous slowing down of a molecular liquid, note that for all of them, specific equipments must be implemented for a given time and space range.

ories. However, one can explore the properties of the supercooled/overcompressed liquid and the glass in a  $P - T$  phase diagram, following isobaric or isothermal paths; the phenomenon is then driven by two thermodynamic control parameters, the temperature and the density which, itself, depends on the temperature. We can then ask the question of their respective contribution to the phenomenon and their coupling. therefore a model-free assessment of the respective contributions of  $\rho$  and  $T$  in the viscous slowing down have been proposed leading to the collapse of all  $\tau_\alpha(\rho, T)$  data on master curves with single density- and species-dependent effective interaction energy  $E_\infty(\rho)$  [17]. As a consequence, the observed crossover from Arrhenius-like to super-Arrhenius behavior is driven by temperature rather than density, which illustrates a major difference with jamming process.

To finish this introduction, before going into the description of organic glasses, it should be noted that there are many empirical formulas to interpolate/extrapolate the dynamic properties with more or less success depending on the temperature range, most of the time using three fitting parameters, see reference [19] for some of them.

## 2. Organic Liquids and Glasses

In Organic Liquids and Glasses, the basic unit is a molecule of size, shape and chemical nature tunable at will. They are most often obtained by cooling a liquid well below its melting temperature ( $T_m$ ) down to the glass transition temperature ( $T_g$ ) at constant pressure with a rate sufficient to avoid crystallization. Depending on systems, some glasses are obtained easily, with no crystallization on cooling, other might require cooling rate as high as  $10^6 - 10^7 K/s$ , (as metallic glasses see this issue); water belongs to this latter case. The intermolecular interactions are of short range van der Waals type of the order of 10 kJ/mol *i.e.* at least 10 times the energy of intramolecular bonding. In some systems another bonding force prevails, the Hydrogen bond of up to few tens of kJ; its energy varies depending on the atoms involved, H-N-O-F, their relative position and distance. For this class of materials, one can define the range of temperature where  $T_g$  is observed experimentally (at atmospheric pressure): the lowest molecular  $T_g$  detected so far by adiabatic calorimetry is the propene ( $C_3H_6$ )  $T_g = 56K$  [21], and the largest are for sugars, as trehalose (393K) or maltohexaose ( $C_{36}H_{62}O_{31}$ ),  $T_g = 448K$ . In the latter cases, large uncertainties in the literature come from a possible hydration of the sugar (for trehalose from 348K to 393K), then  $T_g$  might decrease by several tens of degrees as water is added [20]. Higher  $T_g$ 's for sugars can be found (up to 470 – 480 K), but in that case they are made of several units, and not anymore a single molecule.

Polymers are another very important class of so-called organic systems; these macromolecules consist of a covalent chain of a large number of subunits or monomers. Linear or branched, cross-linked or not, rigid or flexible, possessing one or more types of monomers, polymers can have many different characteristics length and times scales (random chain, Kuhn length, monomer). Each of these lengthscales is associated with specific dynamics, such as large-scale relaxations (reflecting collective responses due to connectivity and entanglement) or very local relaxation processes related to the chemical structure of the monomer. The properties of a polymer are determined by an additional control parameter, the molecular weight  $Mw$  (also referred to as the number of monomers  $N$ ) [24]. At atmospheric pressure, it is known that the density and the glass transition temperature vary inversely with the molar mass:  $T_g = A + \frac{B}{Mw}$ , it expresses the fact that the number of end groups sensitive to free volume decreases as  $Mw$  increases, leading to an increase in  $T_g$ . This increase varies from one polymer to another. Some extreme cases are polystyrene (PS) and polyisobutylene (PIB) : in the case of PS, the variation is as large as 130 degrees from the  $N=7$  to  $N=2000$  monomers accompanied at  $T_g$  by a decrease in the density and in the  $C_p$  jump; at variance for PIB, the variation of  $T_g$  is only of about 13 – 16 degrees for roughly the same change in mass. Due to their larger weight (at least with few monomers) their glass transition temperature is slightly shifted when compared to molecules, the lowest  $T_g$  being for the Polydimethylsilane (PDMS, 130 K) to more than 400 K (Polycarbonate 420K, PolyAcidemethacrylic 501K). Although the  $1/M$  law is robust, it is sometimes necessary to complete it by adding the contribution of the various components of the monomer, like alkyl side chains [25]. Since the glass transition of a polymer is observed at the monomer scale, it keeps a great similarity with that of molecular liquids:  $T_g$  depends on thermal history, with a heat capacity jump, a drastic increase of the relaxation time or viscosity in the melt which obeys similar empirical formula (the most known is the Williams-Landel-Ferry that can be converted to the VTF), GHz-THz signatures of the glassy state [26]. However, the analogy has some limits due to the role of the chain at larger scale : only in very few cases crystallisation is observed, the heat capacity jump is smaller, the dynamical range is also smaller (10 – 11 decades) in the melt due to possible degradation at high temperature.

For molecular liquids the  $T_g$  value changes as well with molecular weight  $M$ , as seen in Figure 2a but in a different way ; one could find a correlation between  $M$  and  $T_g$ ,  $T_g \propto M^{0.6}$  (dashed

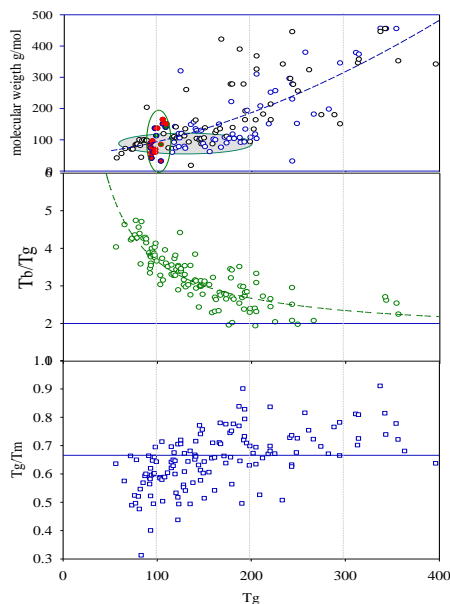


**Figure 2.** molecular properties and glass transition location: a) molecular weight of liquids as a function of their  $T_g$ , a trend is given by the dashed indicating a power law dependence  $M \propto T_g^{1.67}$  ( or  $T_g \propto M^{0.6}$ ). However, many liquids with similar  $T_g$  (red zone) or with the same  $M$  (grey zone) do not support this relation; b) the ratio  $\frac{T_b}{T_g}$  as function of  $T_g$  for the same set of liquids when  $T_b$  is available, the blue line indicates a ratio equal to 2, the dashed line illustrates how the ratio increases at low values of  $T_g$  ; c) the ratio  $\frac{T_g}{T_m}$  as function of  $T_g$  for liquids that crystallise, the line indicates the 2/3 rule. Most data are from [27]

line on the figure) ignoring the specific intermolecular interactions. However, there is a very wide dispersion of points :  $T_g$  might vary a lot with liquids of similar  $M$  (grey zone in the figure), or liquids with the same  $T_g$  might have a huge difference in  $M$ , as cumene ( $T_g=125\text{K}$ ,  $M=120.2$ ) and tetrabutyl orthosilicate ( $T_g=124\text{K}$ ,  $M=320$ ). Note that it does not exclude possible relation within a given chemical serie such as alkanes, polyalcohols [27] as soon as the interactions are kept close; note also that water is an exception here with the lowest  $M$  ( $=18$ ) and  $T_g$  in the literature of  $136\text{K}$  illustrating the tremendous importance of the H-bond network.

Finally, one should note that proteins have a so-called dynamic transition between 180 and 230K, but not properly speaking a glass transition (no  $C_p$  jump detected), distinct from the denaturation temperature; its signature corresponds to an enhanced mobility and a rapid increase of the mean-square displacement as measured by neutron scattering at 1-4 nsec. For globular proteins, the dynamic transition is related to internal dynamics and often melting of frozen water trapped inside or at the surface, [28], which might enhance enzymatic activity.

### 2.1. Empirical rules for the Glass Formation ability and $T_g$ location

In Figure 2b and c, one can find several empirical rules of thumb that help to locate the glass transition temperature of a liquid. In a rough approximation,  $T_g$  increases as  $T_b$  increases [29], changing with the size of the molecule and its interaction strength. However this is just a trend [23] and it does not apply to isomers, when the molecular structure change and the entropic

effects become dominant. At least the ratio  $\frac{T_b}{T_g}$  is always larger than 2 for all the liquids collected here with a strong increases for low  $T_g$ 's ; this ratio might be considered as a liquid range index, which surprisingly increases as the glass transition temperature decreases. Another widely used ratio is the  $\frac{T_g}{T_m}$  supposed to obey the *2/3 rule*. However, in Figure 2c, a large dispersion of points is observed and the rule is not valid for liquids having a value of  $T_g$  below 150K, with notable extremes cases like cycloheptane (0.31) or sucrose benzoate (0.91). It is implicitly assumed with these plots, that a  $T_g$  exists. Moreover very good glass-formers liquids, that do not have a melting point at atmospheric pressure ( m-fluoroaniline, dibutylphthalate ), or others very bad glass-formers, without a known  $T_g$  (methane, Argon, carbone disulfide, benzene..), are not recorded here; it also excludes all cases that are vitrified under specific conditions, for which the rule does not work (water), and illustrates how melting is decoupled from the glass formation. One can apply these rules when the glass transition temperature of a liquid is not known; however it does not predict if it is able to vitrify or not.

A useful rule proposed in the litterature to define the ability of a molecular liquid to form a glass under standard cooling rates is the ratio  $\frac{T_b}{T_m}$  which should be equal or larger than 2; if we take into account the ratios defined above, one can see that the lower limit of this condition must be rather of the order of 4/3. If one now looks at systems plotted in Figure 2, they all follow this rule, even water obtained from hyperquench or compression procedures, or liquids trapped in emulsions, microemulsions, hard confinement (benzene is an example [30] in Figure 6a). One can ask oneself the interest of this type of rule, with which there is finally only the perfect gases that are excluded or more positively think that all liquids can vitrify as soon as a good trick to avoid crystallisation.

So what is a good glass-former ? A system for which crystallisation can be avoided on cooling. The mechanisms (nucleation and growth) of crystallization remain central to define an ability to vitrify or not. Nucleation of crystalites in competition with liquid local order might not perturb the dynamics until it they grow, and the crystal growth rates in highly viscous liquids present usually a maximum at  $1.2 - 1.3 T_g$ . Thus a liquid can maintain in its supercooled state (below  $T_m$ ) for very long times. The kinetic and thermodynamic aspects are widely studied in the literature establishing a possible link between the viscosity, the surface morphology of the grain and the crystal growth [31].

## 2.2. Structure of Organic Glassforming Liquids

The dramatic change in characteristic times of the dynamics is not accompanied by any measurable signature in the structure or remarkable increase in a static correlation length in the pair correlation function. Indeed, the static structure factor  $S(Q)$  changes from one liquid to another because of their distinct molecular shape. This is shown in Figure 3a for a serie of aromatic liquids over a large wave vector ( $Q$ ) range at atmospheric pressure and ambient temperature.  $S(Q)$  can be splitted into an intramolecular form factor  $F(Q)$  acting at high  $Q$  describing the intramolecular contribution and an intermolecular contribution  $D(Q)$  at low  $Q$ 's , *i.e.* larger distances whose Fourier transform gives the intermolecular pair correlation function  $g(r)$  in real space and the local organisation of the first coordination shell.  $D(Q)$  is a linear combination of many partial intermolecular atom-atom structure factors and contains all information of the short and medium range order around a molecule. However, the structure factor  $S(Q)$  as function of  $T$  down to the glass transition, or as a function pressure at constant temperature up to  $P_g$ , exhibits only a smooth evolution with a shift to higher wave vectors due to a density increase and a slight change in shape due to the different temperature dependences of the partial structure factors see Figures



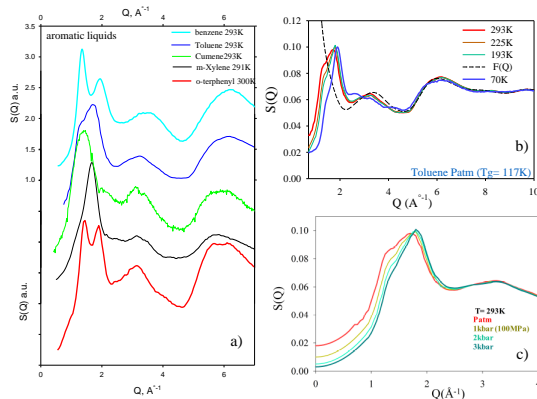


**Figure 3.** Static Structure factor of a serie of aromatic molecular liquids as a function of the wave vector  $Q$  and its dependence on temperature pressure and density, the systems are deuterated and measurements by neutron scattering: a) benzene ( $T_g$  120K confined in microemulsion, Toluene  $T_g = 117$ K, isopropyl benzene or cumene  $T_g = 125$ K, m-xylene  $T_g = 125.5$ K), ortho-terphenyl  $T_g = 245$ K); b) Temperature dependence of  $S(Q)$  of toluene at atmospheric pressure from above  $T_m$  to below  $T_g$ , in addition the form factor  $F(Q)$  of the molecule is shown for its contribution at large  $Q$ 's ;c)  $S(Q)$  changes with pressure along an isotherm . All data were obtained by neutron diffraction on deuterated samples on the diffractometer 7C2 at the Laboratoire Léon Brillouin, Saclay; details on the data traitement are given in [32].

3b and c [32]. Figure 4 a and b illustrate how the main peak of  $S(Q)$  and the short range order remains constant at constant density whatever is the temperature and the changes of the relaxation time or the effective activation energy; this is verified for van der Waals molecular liquids and polymers. Discernable supramolecular ordering at the scale of few nanometers, can only be found in systems sensitive to self-organisation such as ionic liquids or hydrogen bonded liquids as soon as this supramolecular organisation is sufficient larger than intermolecular distance. Figure 4c shows the emergence of a 'prepeak' at lower  $Q$ 's due to the emergence in the liquid of H-bond induced clusters, and how it is sensitive to temperature. In the latter case, one should notice that despite some analogy between the prepeak observed here and the so-called first sharp diffraction peak observed in silica, representing an intermediate range order, its interpretation and  $T$ - $\rho$  dependence is very different.

Finally we should note that even if often the Bragg peaks of the corresponding crystal are located around the position of the main peak in the liquid, the latter does not correspond to a simple broadening of the Bragg peaks because of the disorder but to very different local structures (the crystal nucleus and the local order of a liquid are not equivalent, except in the case of water).

### 2.3. How to change $T_g$ of a given system?

For a given liquid, several values of  $T_g$  can be found, depending on its definition and the experiments carried out (see above): for example, in calorimetry by changing the cooling and/or heating rates, which is equivalent to change the relaxation time of the liquid between 10 and 1000s when equilibrium is reached (it should be kept in mind, however, that the most unambiguous

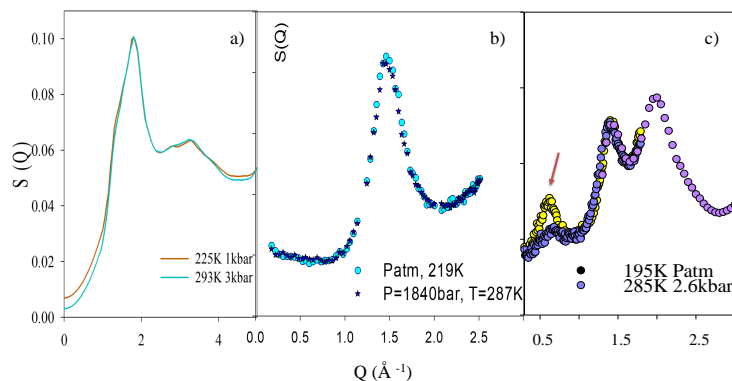


**Figure 4.** Static Structure factor along an isochore  $T$  and  $P$  are indicated in the plot: a) a van der Waals liquid, toluene  $\rho = 1.06\text{g/cm}^3$ ; b) a polymer, polubutadiene,  $M_w=7000$ ,  $\rho = 0.94\text{g/cm}^3$ ; c) an hydrogen bonded liquid m-fluoroaniline  $\rho = 1.3\text{g/cm}^3$ , here the arrow indicates the position of a prepeak due to the presence of H-bond induced clusters and its  $T$ -dependence associated with the strength of the H-bond.

definition of the glass transition temperature is the one made during cooling). Even if the time scale of the measurement is less than the relaxation time and the system is apparently frozen in the glassy state, its thermodynamic properties continue to evolve at least down to temperatures where equilibrium cannot be reached even for the longest annealing times. This amounts to defining a so-called "fictive" temperature, *i.e.* the temperature at which the value of the thermodynamic properties (such as density or entropy) of the glass would be equivalent to their equilibrium value in the liquid. However in order to vary the value of  $T_g$  with the same definition of characteristic time, it is necessary to change the thermodynamic path or impose an additional constraint, while always avoiding crystallization. Thus, for a given system, keeping the same intermolecular interactions, we can modify the transition temperature by changing the pressure and thus define a glass transition line in a pressure-temperature diagram as for the lines of fusion or evaporation of the system. The properties of the supercooled and overcompressed liquid can be studied along isobars (with  $T_g(P)$ ) or isotherms defining the glass transition pressure  $P_g(T)$  [35] or along isochores when the  $P$ - $V$ - $T$  equation is known. The Figure 5 illustrates the different approaches of the glass transition line in a  $P$ - $T$  phase diagram, how the dynamical properties evolve along different thermodynamical paths. It brings us to the question about the respective role of the various external control parameters, temperature  $T$ , pressure  $P$ , density (or volume  $V$ ) in the viscous slowing down of glass forming liquids and polymers [36]. One can observe for experiments performed at constant pressure that the role of temperature becomes more important in the super-Arrhenius regime as one approaches the glass transition than the density, which contribution is more significant at high temperatures. Moreover, similarly to the analysis of dynamical heterogeneities at atmospheric pressure close to  $T_g$ , the number of molecules involved in dynamical heterogeneities could be evaluated in the whole phase diagram.

Another way to modify the glass transition of a given system is to confine it at nanoscale. It was first considered as an extra trick to avoid crystallisation in liquids prone to crystallise : the use

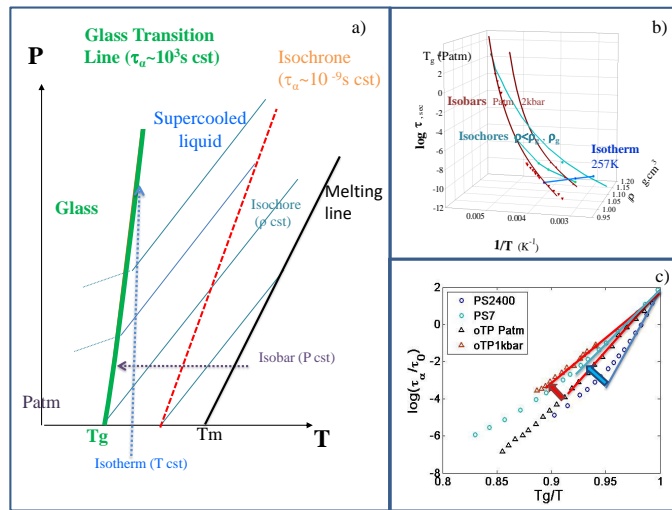


**Figure 5.** Supercooled and overcompressed liquid : a) Pressure-Temperature phase diagram with  $T_g$  line and melting line, illustrating the different thermodynamic paths, that can be used to obtain a glass, crossing the  $T_g$  line; this line is an 'isochronic' line, *i.e.* a constant relaxation time line, other similar lines can be defined in the diagram for shorter relaxation times; b) 3D plot of the relaxation time of m-toluidine as a function of temperature and density with the different thermodynamical paths; c) relaxation time as a function of temperature rescaled by  $T_g$  for a molecular liquid (o-terphenyl) at two different isobars and for a polymer (polystyrene) for two molecular weight  $Mw$  [33], the straight lines indicate how the fragility index is calculated and the arrows how the fragility evolves for a molecular liquid, o-terphenyl, when the pressure changes (in red) or for a polymer, polystyrene, with different molecular weight (in blue).

of microemulsions stable in time and in temperature allows the formation of glass with liquids such as benzene,  $CS_2$  or  $CCl_4$  [41]. Many experiments and simulations focussed on the effect of geometrical confinement on phase transitions, thermodynamics and dynamics of liquids. Restricted geometries have significant consequences on first order phase transitions (such as melting/freezing or solid-solid), but also in the glass formation [42]; phase transition pressures and temperatures are often shifted from the bulk values and new phases can appear due to surface forces. Thus another phase diagram  $T - D$  can be considered where  $P$  in the previous one is replaced by the size of the confinement ( $D$  the pore diameter of the material), as illustrated in Figure 6. The study of the glass transition of confined liquids has been largely promoted on one hand by the idea that the geometrical restriction in the range 1–10 nm should compete with characteristic length scales responsible of the viscous slowing down, and, on the other hand, by the progress made in the synthesis of micro-mesoporous materials. Although the decrease of the melting temperature as the pore size decreases is robustly described by the Gibbs-Thomson equation, no satisfactory consensus has been found to predict experimentally the evolution of  $T_g$  with the pore size. Several experimental difficulties arise: the filling conditions, the existence of structural heterogeneities induced by the confinement, the distribution of the relaxation time between a solid wall and the center of the pore and finally, the ambiguous distinction between a crystalline nanograin and a glass. In order to conclude on finite size effects on the dynamics and on the quantification of a dynamic length, it is thus necessary to control concomitant effects

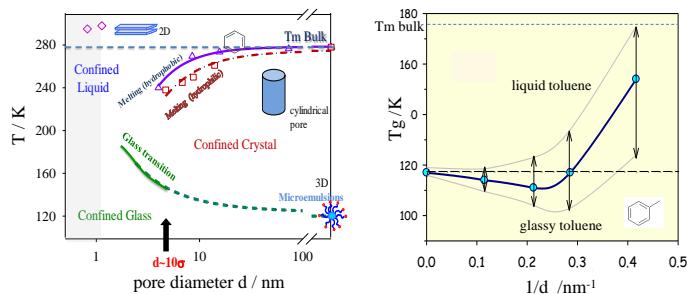


**Figure 6.** Temperature-Pore Diameter phase diagram of confined liquids : a) case of a liquid prone to crystallize, benzene  $C_6H_6$ . The melting temperature is reduced according to the Gibbs Thomson law; in the smallest pores ( $d < 10 \times$  molecular size), the confined liquid no longer crystallizes but rather exhibits a glass transition. A "pseudo" bulk  $T_g$  is obtained in quenched microemulsions with large pore size [30] ; b) Glass transition temperature of toluene versus the inverse of the pore diameter, the line is the calorimetric glass transition temperature defined at the maximum of the heat capacity derivative ; the arrows represent the widths of the transition region increasing as the pore size decreases ; the dashed line refers to  $T_g$  and  $T_m$  of the bulk toluene [32].

due to the presence of an interface and the nature of the wall-liquid interaction; indeed  $T_g$  can decrease, increase or remain constant depending on these fluid-wall interactions and its consequences on the local organisation of the liquid. So far, the study of the glass transition under confinement does not allow the extraction of an intrinsic correlation length associated with the viscous slowing down approaching  $T_g$ , but it reveals the important role of matrix-adsorbate interactions and the competition between finite size effects and surface effects. However, thanks to the huge surface to volume ratio that nanopores offer, knowing how thermodynamics and dynamics of fluids are affected by confinement is of great importance for many applications and a better understanding in lubrication, adhesion, nanotribology, fabrication of other nano-materials etc...

### 3. Concept of Fragility

At the Blackburg Workshop in 1984 , then in a published paper in 1985 [37], C.A. Angell proposed to compare and rank the liquids according to their fragility index  $m$ , *i.e.* their departure from an Arrhenius behavior;  $m$  characterises how quick in temperature the dynamics and the thermodynamics change above  $T_g$ . This index was first defined close to  $T_g$  as  $m = \partial \log_{10}[\tau(T)/\tau_\infty] / \partial(T_g/T)|_{T_g}$ , for liquids studied at normal pressure. ( Note : fragile is distinct from brittle ). In a logarithmic representation, the relaxation or the viscosity of different liquids are plotted as function of  $T_g/T$ , thus converging at a single point  $T_g/T = 1$  corresponding to the time of the chosen definition for the glass transition temperature, generally 100–200s ( see figure

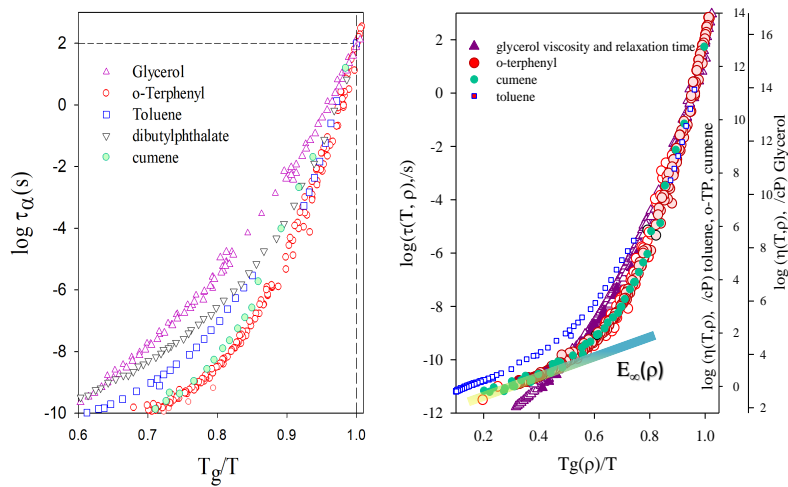


**Figure 7.** dynamics of organic liquids and fragility : left, the so-called Angell's plot, relaxation time and viscosity of various liquids at atmospheric pressure from high temperature to  $T_g$  defined by  $\tau=200s$ ; right, relaxation time and viscosity of the same liquids rescaled by  $T_g(\rho)/T_g$ .

5c and 7a ). The  $T_g$  scaling was already suggested several years before [38], however when Angell introduced the fragility concept, he went a step further and claimed that : “The temperature dependence of the average relaxation time as well as the detailed relaxation function seem to be closely connected with the nature of the intermediate range order. Thus, structural relaxation is the first of our glass science problems identified as involving the intermediate range order” [37], in an attempt to correlate dynamics with the thermodynamic behavior and local order. Accordingly, strong liquids are those with a low value of  $m$  and a pseudo tetrahedral structure , (about 16 for the strongest as silica, it is assume that  $\log_{10}[\tau_\infty] = -14$ ), while the most fragile ones have a higher value, up to 200 for some high  $Mw$  polymers ( polystyrene,  $m = 139$  ; poly(vinyl chloride),  $m = 191$ ). For molecular liquids it varies in a more narrow range from about 50 (glycerol, 53) to 90 (salol,  $m=73$ , oTP,  $m=80$  ). Higher fragilities for molecular liquids can be found (sorbitol, decaline [40], etc.. above 130 ) ; however in all cases additional features such as mixtures, or specific behavior of H-bond network, or how the slope is calculated, might explain the high values. Differences in the temperature dependence of the relaxation time of liquids are sometimes quantified through other indices like the thermodynamic fragility [43] compared to the kinetic one, referring to the  $C_p$  jump or the change of the configurational entropy. The classification was extended to many different categories of systems : polymers, plastic crystals, and spin glasses [44]. It was also suggested to extended the classification from close to  $T_g$  up to higher temperatures close to the melting temperature : the former index fragile *vs* non-fragile to measure how much the viscosity is Arrhenius-type at low temperature while the second one strong *vs* weak does the same around the melting point.

### 3.1. *Isobaric versus Isochoric Fragility*

We have learned from the experiments carried out under high pressure that to a large extent temperature is the driving parameter for viscous slowing down close to  $T_g$ , thus challenging a large number of existing models predicting a preponderant role of density via congestion effect and a decrease of the free volume. The contribution due to the density can be reduced to a single parameter, an effective activation energy  $E(\rho)$  that is extracted from the data at high temperature, *i.e.* in a liquid and Arrhenius-like regime. Thus the simplest description of  $\tau(T, \rho)$  can be reduced from  $\tau_\alpha(\rho, T) = \tau_\alpha^\infty(\rho) \exp[E(\rho, T)/T]$  to  $\tau_\alpha(\rho, T) = \tau_\alpha^\infty(\rho) \exp[E_\infty(\rho)/T]$ . Accordingly, all isochoric data should collapse onto a master curve [17]: the density scaling has been verified for many systems from molecular liquids to polymers and even ionic liquids. It was confirmed by many groups using different probes, viscosity, dielectric spectroscopy, NMR, Neutron scattering [18]. Different functional forms are possible for describing the density dependence of  $E(\rho)$ , among them the power law dependence  $\rho^x$ , reminiscent of models of monodisperse soft spheres interacting through a power-law pair potential, seems to fit quite well the data. When only high viscosity or long relaxation times are available, without high temperature data to evaluate the effective activation energy  $E(\rho)$  in absolute unit, then the scaling in terms of  $e(\rho) \propto \rho^x$  works equally well as shown with polymers. The exponent  $x$  of the power law varies from one liquid to another one, between less than 1 (sorbitol  $x=0.13$ ) to 8 (toluene), and is not always constant over a large pressure-density range. So far it was not checked for strong and inorganic liquids. The physical interpretation of this density scaling remains to be understood but new approaches such as the Isomorph theory tends to rationalise it [45]. In addition, one should stress that the Arrhenius behavior proposed for the high-T liquid has also no satisfactory theoretical explanation.

The density scaling has two major consequences. First, one can revisit the concept of fragility defined originally at constant pressure and introduce the isochoric fragility  $m_\rho$ :  $m_\rho = \left. \frac{\partial \log(\tau_\alpha)}{\partial (T_g/T)} \right|_\rho$  ( $T = T_g$ ), here defined at the glass transition temperature at which  $\tau_\alpha$  has a given value at a given  $\rho$ . While the isobaric fragility includes the effects of temperature and density, the isochoric one is independent of density whatever is the density range explored. Thus, the isochoric fragility, *i.e.* the measure of the degree of super-Arrhenius behavior at constant density, must be taken as an intrinsic property of a given glassformer. The second consequence of the density scaling is a modified Angell plot as illustrated in Figure 7 b. The Angell plot defining the isobaric fragility represents  $\log(\tau_\alpha)$  versus the inverse scaled temperature  $T_g/T$  at constant (usually atmospheric) pressure in Figure 7 a. Instead, one can plot  $\log(\tau_\alpha)$  versus  $T_g(\rho)/T$ , where all T- $\rho$  data of a specific liquid collapse and can be compared to another one. The steepness of the  $\log(\tau_\alpha)$ -vs- $T_g(\rho)/T$  curve is a measure of the intrinsic fragility of a system. One can notice that in the standard Angell plot, all the liquids have a different behavior and a different isobaric fragility, while in the isochoric Angell plot, the liquids exhibit a similar isochoric fragility when the glass transition is approached.

### 3.2. *correlations between slow and fast dynamics*

The Angell classification and the fragility index was intensively used in order to rationalise the rich phenomenology observed in supercooled liquids and glasses. A number of correlations have been proposed between fragility and other properties related to the glass transition to extract important features and improve models or theories. The properties of liquids and polymers have been investigated mainly at atmospheric pressure and plotted as a function of the isobaric  $m_p$ , neglecting the possible specific dependence on temperature or density. From the supercooled liquid side,  $m_p$  was correlated to the stretching exponent of the relaxation, the heat capacity jump or the decrease of the configurational entropy. From the glass side, properties are measured

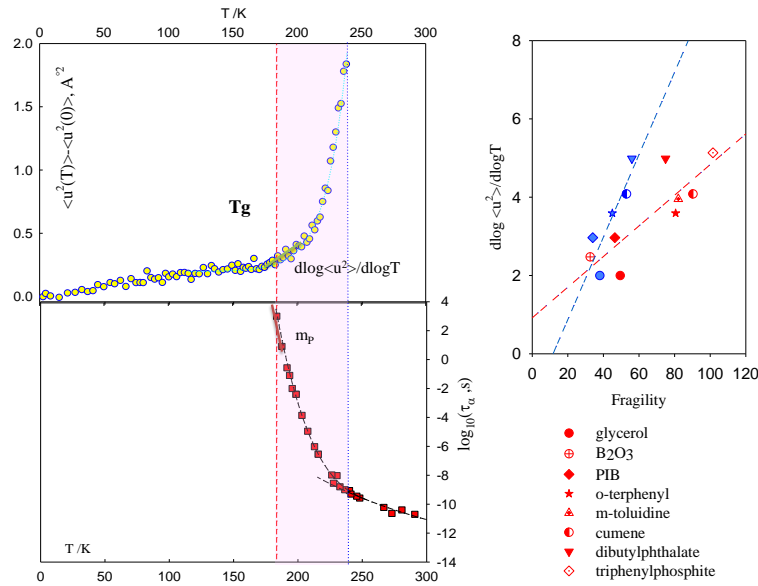


**Figure 8.** correlation between slow and fast dynamics of m-toluidine: left) top , mean square displacement at 4 nanoseconde (msd) as measured by neutron scattering; bottom, corresponding structural relaxation time at atmospheric pressure; slightly above  $T_g$  defined at  $\tau=200\text{s}$ , the pink area shows the respective change of the dynamics and of the msd ; right) correlation between the slope at  $T_g$  of the msd and isobaric in red and isochoric fragility in blue of different liquids given in the figure.

at very short times as for any solids and compared to the very slow dynamics above  $T_g$ . Among many properties, we can mention the relative intensity of the Boson peak observed by light or neutron scattering in the meV range, which appears directly related to the fragility of the system: the stronger the system, the greater the intensity. In this case the correlation with the isochoric fragility is comparable suggesting that the Boson peak intensity could be related to the effect of temperature on the dynamics and the super-Arrhenius behavior above  $T_g$ . Another proposed correlation involve the ratio of elastic to inelastic signal in the X-ray Brillouin spectra, also defined as the non-ergodicity factor. At variance to the previous case, the correlation becomes very poor when the isochoric fragility is considered [47] and better related to density effects and the variation of  $E(\rho)$  from one system to another one.

The correlations are critical to understanding the consequences of super-arrhenic behavior on the properties of glasses, establishing a link between solid and liquid models. Conversely, this raises the question of how properties probed on the pico-nano second time scale might determine slow processes observed over hours. A convincing example is given in Figure 8 for a molecular liquid, where the mean square displacement (MSD) measured at a fixed time of 4 nanosecond and the structural relaxation evolve with temperature in the glass transition domain : as shown, the larger MSD is related to the shorter relaxation time . It was first observed in 1992 by Buchenau and Zorn for Selenium, and generalise to all systems studied so far. Moreover the change in MSD just above  $T_g$  and the fragility, either  $m_p$  or  $m_p$  (Figure 8 right), is more pronounced for the most fragile systems, as predicted by elastic models. One should note that the correlation holds for MSD taken at the ns timescale, but fails when the msd is measured

at the ps timescale and includes the vibrational contributions. Finally, one can always argue that correlation does not mean causality but a full understanding of the glass-transition must encompass both fast and slow dynamics.

#### 4. conclusion

In this short review, the properties of organic glass forming systems are presented in a non exhaustive way. Organic glasses constitute a very large and important category of materials with implications in many different fields where dynamical arrest takes place. The temperature range over which the glass transition is observed is compared to other glass forming liquids, as well their chemical composition with  $T_g \propto Mass^{0.6}$ ; some rules of thumb to locate  $T_g$  or define their ability to vitrify are discussed according to different thermodynamic paths or external constraints. The most remarkable property of these liquids is how fast in temperature their viscosity or structural relaxation time increases as approaching  $T_g$  which is also described as super-Arrhenius behavior. To characterize this behavior and rank the liquids of different strength, C.A. Angell introduced the concept of Fragility nearly 40 years ago. He proposed to classify liquids as fragile or strong in an Arrhenius plot with  $T_g$  scaling, the most fragile demonstrating the fastest changes in the dynamical properties. Originally considered only at atmospheric pressure, the study can be extended in a wider T-P range focussing on the specific contributions of temperature or density. At zeroth-order, the viscous slowing down is then shown to be best described as a thermally activated process, whose super-Arrhenius behavior is not primarily driven by congestion effects due to lack of free volume. Moreover all  $\tau(\rho, T)$  or  $\eta(\rho, T)$  data collapse by placing the data on master curves that depend only on a single density- and species-dependent effective interaction energy (independent of T),  $E_\infty(\rho)$ , expressing the quantitative role of the density. This led to propose a modified version of the Angell plot, the isochoric Angell plot. However the most important consequence of the master curve obtained by scaling out the density dependence of the relaxation time is the introduction of an intrinsic property to each substance, the isochoric fragility  $m_\rho$ . All the correlations between the glass properties below  $T_g$  and the viscous slowing down just above  $T_g$  can be reconsidered by taking the isochoric fragility instead of the isobaric one.

The last considerations suggest that there are still two areas that may need further attention. First at very long relaxation times scrutinizing what happens between  $T_g$  and  $T_K$ , this has been proposed recently with highly stable glasses prepared by physical vapor deposition [48]. This procedure discovered by Ediger and his group provide new insights into properties of a possible ideal glass bypassing the kinetic problem of long aging. Such vapor deposition preparation techniques seem to be very promising, both in terms of understanding aging phenomena and in the preparation of new materials more thermodynamically and kinetically stable than those obtained through standard cooling rates. The second area is at higher temperatures, where the dynamics of glass-forming molecular liquids is well described by an Arrhenius temperature dependence with a sizable apparent activation energy  $E_\infty(\rho)$ . It raises the question of why the high temperature liquid dynamics of glassforming molecular systems is dominated by thermally activated processes (of several  $k_B T$ ) and the possible location of a reference temperature (or energy) large compared to the melting temperature setting the scale for the activation energy.

#### References

- [1] C. A. Angell, *Science* **267**, 1924–1935 (1995). C. A. Angell, J. M. Sore, and E. J. Sore, *The Journal of Physical Chemistry*, **82**, (24), 2623 (1978).
- [2] J. C. Dyre, *Rev. Mod. Phys.*, **78**, 3, 952-972 (2006).



- [3] S. R. Forrest and M. E. Thompson, *Chem. Rev.* 107, 923 (2007); M. D. Ediger and Peter Harrowell, *J. Chem. Phys.* 137, 080901 (2012).
- [4] A. Keiichiro, H. Suga, S. Seki, *Bulletin of the Chemical Society of Japan*, 41(5), 1073-1087, (1968). F. Affouard, M. Descamps, *Phys. Rev. E*, 72, (1), 012501, (2005)
- [5] T. Hecksher, DH Torchinsky, C Klieber, JA Johnson, JC Dyre, KA Nelso, *Proc Natl Acad Sci USA*, 114(33), 8710-8715, (2017); Jensen, M. H., Gainaru, C., Alba-Simionesco, C., Hecksher, T., and Niss, K., *Phys. Chem. Chem. Phys.*, **20**, 1716-1723 (2018).
- [6] D. Kivelson, S. A. Kivelson, X.-L. Zhao, Z. Nussinov, and G. Tarjus, *Physica A* **219**, 27 (1995); D. Kivelson, X.-L. Zhao, G. Tarjus, and S. A. Kivelson, *Phys. Rev. E* **53**, 751 (1996).
- [7] B. Schmidtke, N. Petzold, R. Kahlau, and E. A. Rössler, *J. Chem. Phys.*, 139, 084504, (2013).
- [8] Proceedings of the Symposium on “Fragility of Glass-forming Liquids”, A. L. Greer, K. F. Kelton, and S. Sastry eds., TRIPS 13 (New Dehli, 2014).
- [9] R. Richert, N. Israeloff, C. Alba-Simionesco, F. Ladieu, D. L’Hôte, Chapter 4 in *Dynamical Heterogeneities in Glasses, Colloids and Granular Materials*, L. Berthier, G. Biroli, J.P. Bouchaud Eds, Oxford University Press, (2011).
- [10] W. Kauzmann, *Chem. Rev.* 43, 219–256 (1948); L. Berthier, M. Ozawa and C. Scalliet, *J. Chem. Phys.* 150, 160902 (2019)
- [11] S. A. Kivelson and G. Tarjus, *Nature Materials* , 7, 831, (2008); L. Berthier and G. Biroli, *Rev. Mod. Phys.* 83, (2011), pp. 587-645; V. Lubchenko and P. G. Wolynes, *Annu. Rev. Phys. Chem.* 58, (2007), pp. 235-266. J. D. Stevenson, J. Schmalian, and P. G. Wolynes, *Nature Physics*, 2, 268-274, (2006); G. Tarjus, “An overview of the theories of the glass transition,” in *Dynamical Heterogeneities and Glasses*, (Oxford University Press, 2011).
- [12] J. H. Gibbs and E. A. DiMarzio, *J. Chem. Phys.* 28, 373–383 (1958); G. Adam and J. H. Gibbs. *J. Chem. Phys.*, **43**, 139-146, (1965).
- [13] L. Berthier, G. Biroli, J.-P. Bouchaud, L. Cipelletti, El Masri D., L’Hote D., F. Ladieu, and Pierno M. *Science*, 310:17971-800, (2005); C. Dalle-Ferrier, C. Thibierge, C. Alba-Simionesco, L. Berthier, G. Biroli, J.-P. Bouchaud, F. Ladieu, D. L’Hote, and G. Tarjus. *Physical Review E*, 76:041510, (2007); L. Berthier, G. Biroli, J.P. Bouchaud, and G. Tarjus, *J. Chem. Phys.* 150, 094501 (2019).
- [14] Cohen, M. H., and Turnbull, D., *J. Chem. Phys.* 31, 1164 (1959); Turnbull, D., and Cohen, M. H., *ibid* 52, 3038 (1970); Grest, G. S., and Cohen, M. H., *Adv. Chem. Phys.* 48, 455 (1981); Gotze, W., and Sjogren, L., *Rep. Prog. Phys.* 55, 241 (1992); 11D. Chandler and J. P. Garrahan, *Annu. Rev. Phys. Chem.* 61, 191–217 (2010); C. P. Royall, F. Turci, and T. Speck, *J. Chem. Phys.* 153, 090901 (2020); G. Kapteijns et al, *J. Chem. Phys.* 155, 074502 (2021).
- [15] G. Biroli and J.-P. Bouchaud *EPL*, 67, 21, (2004)
- [16] J.-L. Barrat [hal.archives-ouvertes.fr/hal-00018118/file/erice1.pdf](http://hal.archives-ouvertes.fr/hal-00018118/file/erice1.pdf) (2006); F. Leonforte, A. Tanguy, J. Wittmer, J.-L. Barrat, *Phys Rev B* 2004, (2005); H. Mizuno, S. Mossa , J.-L. Barrat, *PROCEEDINGS OF THE NATIONAL ACADEMY OF SCIENCES*, 111 ,33, (2014). F. Casas, C. Alba-Simionesco, H. Montes, F. Lequeux, *Macromolecules*, 41 , 860-865 (2008); L. Hong, V. N. Novikov, and A. P. Sokolov, *Phys. Rev. E* 83, 061508 (2011); D. Fragiadakis, R. Casalini, and C. M. Roland, *Phys. Rev E* 84, 042501 (2011).
- [17] Alba-Simionesco, C., Kivelson, D. Tarjus, G., *J. Chem. Phys.* 116, 503, (2002); Tarjus G., Kivelson D., Mossa S., and Alba-Simionesco C. *Cond-Mat/0309579v1 25sep 2003*, *J. Chem. Phys.* 120, 6135 (2004); Alba-Simionesco C., Caillaux-Chauty A., Alegria A., Tarjus G., *Europhys. Lett.* 68, 58-64, (2004); Alba-Simionesco C., Tarjus G., *Journal of Non-Crystalline Solids: X*, Volume 14, 100100, ISSN 2590-1591,(2022).
- [18] C. M. Roland, S. Hensel-Bielowka, M. Paluch, and R. Casalini, *Rep. Prog. Phys.* 68, (2005), pp. 1405-1478; M. Paluch, S. Haracz, A. Grzybowski, M. Mierzwa, J. Pionteck, A. Rivera-Calzada, and C. Leon, *J. Phys. Chem. Letters* 1, pp 987-992, (2010); H. Wase Hansen, F. Lundin, K. Adrjanowicz, B. Frick, A. Matic, and K. Niss, *Phys. Chem. Chem. Phys.* 22, pp. 14169-14176, (2020).
- [19] Vogel, H. *Phys. Zeit.* 22, 645–646 (1921); Fulcher, G. S., *J. Am. Ceram. Soc.* 8, 339–355 (1925); Tammann, G. *J. Soc. Glass Technol.* 9, 166–185 (1925); Bassler, H. *Phys. Rev. Lett.* 58, 767–770 (1987); Hecksher, T., Nielsen, A., Olsen, N. et al. *Nature Phys* 4, 737–741 (2008); J. C. Mauro, Y. Yue, A. J. Ellison, P. K. Gupta, and D. C. Allan, *Proc. Natl. Acad. Sci. USA*, 46, 19780 (2009); V. N. Novikov, A. P. Sokolov, *Phys. Rev. E* 92, 062304, (2015); J. Krausser, K. H. Samwer, and A. Zaccone, *Proc. Natl. Acad. Sci. U. S. A.* 112, 13762 (2015).
- [20] Alexandra Simperler, Andreas Kornherr, Reenu Chopra, P. Arnaud Bonnet, William Jones, W. D. Samuel Motherwell, and Gerhard Zifferer, *The Journal of Physical Chemistry B* 2006 110 (39), 19678-19684; Yrjö Roos, *Carbohydrate Research*, Volume 238, Pages 39-48, 1993; Sebastian Linnenkugel, Anthony H.J. Paterson, Lee M. Huffman, John E. Bronlund, *Food Hydrocolloids*, Volume 128, 107573, 2022.
- [21] S. Tatsum, S. Aso, O. Yamamuro, *Phys Rev Lett.* 109(4), 045701 (2012).
- [22] K.D. Roe and T.P. Labuza *International Journal of Food Properties*, 8, 559–574, (2005); S. Linnenkugel, A. H.J. Paterson, L. M. Huffman, J. E. Bronlund, *Food Hydrocolloids*, 128, 107573,(2022).
- [23] C. Alba-Simionesco, J. Fan, C. A. Angell *J. Chem. Phys.* 110, 5262-5272 (1999); L.-M. Wang and R. Richert, *J. Phys. Chem. B* 2007, 111, 3201-3207.
- [24] Ferry, J. D. *Viscoelastic Properties of Polymers*, 3rd ed.; John Wiley and Sons, New York, (1980). B. Frick, D. Richter, *Science*, 67, (1995). S. Napolitano, E. Glynos and N.B. Tito, *Rep. Prog. Phys.* ,80, 036602, (2017).

- [25] Xie, R., Weisen, A.R., Lee, Y. et al. *Nat Commun* 11, 893 (2020).
- [26] macromol polymers, boson McKenna
- [27] L.-M. Wang and R. Richert, *J Phys. Chem. B*, 111 (12), 3201-3207, (2007) K. Wynne, private communication at PNCS16; W. Ping, D. Paraska, R. Baker, P. Harrowell, C. A. Angell, *J Phys. Chem. B*, 115 (16), 4696-4702, (2011); V.N. Novikov, E.A. Rössler, *Polymer*, 54 (26), 6987-6991, (2013).
- [28] Doster, W., Bachleitner, A., Dunau, R., Hiebi, M., Luscher, E. *Biophys. J.* 50, 213-219, (1986); Parak, F., Heidemeier, J. Nienhaus, G. U. *Hyperfine Interac.* 40, 147-157, (1988); Iben, I. E. T., Braunstein, D., Doster, W., Frauenfelder, H., Hong, M. K., Johnson, J. B., Luck, S., Ormos, P., Schulte, A., Steinbach, P. J., Xie, A. H. Young, R. D. *Phys. Rev. Lett.* 62, 1916-1919, (1989); Frauenfelder, H., Sligar, S. G. Wolynes, P. C. *Science* 254, 1598-1603, (1991). (London) 357, 423-424. Smith, J., Kuczera, K Karplus, M. (1990) *Proc. Natl. Acad. Sci. USA* 87, 1601-1605.
- [29] D. Turnbull and M. H. Cohen, *J. Chem. Phys.* 29, 1049, (1958). C. Alba-Simionesco J. Fan, C. A. Angell *J. Chem. Phys* 110, 5262-5272 (1999).
- [30] G. Dosseh, Y. Xia, C. Alba-Simionesco, *J. Phys. Chem. B* 107, 26, 6445-6453, (2003); D. Morineau, C. Alba-Simionesco, *J. Chem Phys.* 118, 20, 9389, (2003).
- [31] Ediger MD, Harrowell P, Yu L. *J. Chem. Phys.* 128, 034709/1-6 (2008).
- [32] Morineau D., Alba-Simionesco C. *J. Chem. Phys.* 109, 8494 (1998); Morineau D., Alba-Simionesco C., Bellissent-Funel M.C., Lautie M.F. *Europhys. Lett.* 43, 195 (1998); PhD Thesis Denis Morineau : Structure de liquides moléculaires fragiles à l'approche de la transition vitreuse par diffusion de neutrons et simulations Monte Carlo, Univ Paris-Sud Orsay (1997).
- [33] J. Hintermeyer, A. Herrmann, R. Kahlau, C. Goiceanu, and E. Rosler, *Macromolecules*, 41(23) :93359344, (2008); Dalle-Ferrier, Cecile; Niss, Kristine; Sokolov, Alexei; Frick, Bernhard; Serrano, Jorge; Alba-Simionesco, Christiane , *Macromolecules*, , 43(21), 8977-8984, (2010); Y. Ding, V.N. Novikov, A. P. Sokolov, A. Cailliaux, C. Dalle-Ferrier, C. Alba-Simionesco, B. Frick *Macromolecules*, 37, 9264-9272, (2004); C. M. Roland and R. Casalini, *The Journal of Chemical Physics*, 119 :1838-1842, (2003).
- [34] M. Descamps, A. Aumelas, S. Desprez, J.F Willart, *Journal of Non-Crystalline Solids*, 407, 72-80, (2015)
- [35] Cailliaux, A., Alba-Simionesco, C., Frick, B., Willner, L. Goncharenko, I. *Phys. Rev. E* 67, 010802, (2003); Frick, B., Alba-Simionesco, C., Andersen, K. Willner, L. *Phys. Rev. E* 67, 51801, (2003).
- [36] M. L. Ferrer, C. Lawrence, B. G. Demirjian, D. Kivelson, G. Tarjus, and C. Alba-Simionesco, *J. Chem. Phys.* 109, 8010 (1998); Ferrer M.L., Sakai H., Kivelson D., Alba-Simionesco C., *J. Phys.Chem. B*, 103 (20), 4191-6, (1999).
- [37] C. A. Angell, in *Relaxations in Complex Systems*, K. L. Ngai and G. B. Wright Eds. (NRL, Washington, 1985), p. 3; *J. Non-Cryst. Solids* 73, (1985), pp. 1-1; *J. Non-Cryst. Solids* 131-133, (1991), pp. 13-31.
- [38] W.T. Laughlin, D.R. Uhlmann, *J. Phys. Chem.* 76 (16), 2317-2325, (1972); D. L. Sidebottom, *J. Non-Cryst. Solids* 524, 119641, (2019).
- [39] Phillips, W. A. *Rep. Prog. Phys.* 50, 1657 (1987); Zeller, R. C., Pohl, R. O. *Phys. Rev. B* 4, 2029 (1971); Parshin, D. A., Schober, H. R., Gurevich, V. L. *Phys. Rev. B* 76, 064206 (2007); Schirmacher, W., Ruocco, G. , Scopigno, T. *Phys. Rev. Lett.* 98, 025501 (2007).
- [40] Wang L.-M., Angell C.A., and Richert R. *J. Chem. Phys.* 125, 074505 (2006); Duvvuri K. and Ranko Richert R., *J. Chem. Phys.* 117, 4414 (2002).
- [41] Dubochet J., Adrian M., Teixeira J. Alba C., Kadiyala K. MacFarlane D. and Angell C. *J. Phys. Chem.* 88 6727-6732, (1984).
- [42] Mataz Alcoutlabi, Gregory B McKenna, *J. Phys.: Condens. Matter* 17 R461 (2005); Alba-Simionesco, C., Coasne, B., Dosseh, G., Dudziak, G., Gubbins, K.E., Radhakrishnan, R., Sliwinska-Bartkowiak, M., *J. Phys.-Condens. Mat.* 18:R15-R68. Topical review (2006); G. Dosseh, C. Le Quellec, N. Brodie-linder, C. Alba-simionesco, W. Haeussler and P. Levitz *J. of Non-Crystalline Solids*, 352,4964-4968, (2006).
- [43] Ito K., Moynihan C.T., Angell C.A., *Nature* 398, 492-495 (1999); Martinez L.M., Angell C.A. *Nature* 410, 663-667 (2001); Wang L.M., Velikov V., Angell C. A., *the Journal of Chemical Physics* 117:22, 10184-10192, (2002); Dyre, J. C., Olsen, N. B. and Christensen, T., *Phys. Rev. B* 53: 2171, (1996).
- [44] J. Souletie et al *J. Physique I (France)* 1, 1627 (1991); GB McKenna G.B., *J. Chem. Phys.*, 114, 13, (2001); Böhmer et al *Journal of Non-Crystalline Solids: X*, 14, 100097, (2022); M. L. Ferrer, H. Sakai, D. Kivelson, and C. Alba-Simionesco, *J. Phys. Chem. B* 103, 4191 (1999).
- [45] J. C. Dyre, *Phys. Rev. E* 88, 042139(2013); R. Casalini, T. C. Ransom, *J. Chem. Phys.* 151, 194504, (2019).
- [46] A.P.Sokolov et al. *Phys. Rev. Lett.* 71, 2062 (1993); T.Scopigno et al., *Science* 302, 849 (2003); V.N. Novikov and A.P.Sokolov *NATURE* 431, 961 (2004); J.C.Dyre, *Nature Mat.* 3, 749 (2004); P.Harrowel et al. *Phys. Rev. Lett.* (2006).
- [47] K. Niss et C. Alba-Simionesco. *Phys. Rev B* 74, 024205 (2006); Niss, K.; Dalle-Ferrier, C.; Tarjus, G.; et al.; *Journal of Physics-Condensed Matter* Volume: 24 Issue: 5 (2012); Niss K., Dalle-Ferrier C., Frick B., Russo D., Dyre J. and Alba-Simionesco C., *Physical Review E*, 82, No.2, (2010)
- [48] S. F. Swallen, K. L. Kearns, M. K. Mapes, Y. S. Kim, R. J. McMahon, M. D. Ediger, T. Wu, L. Yu, and S. Satija, *Science* 315, 353-356 (2007) ; M. D. Ediger, *J. Chem. Phys.* 147, 210901 (2017).